Annonaceous acetogenins mimic AA005 targets mitochondrial trifunctional enzyme a subunit to treat obesity

Li-Shun Wang (lishunwang@fudan.edu.cn)
Fudan University
Bing Han
Key laboratory of whole-period monitoring and precise intervention of digestive cancer (SMHC)
Zhan-Ming Li
Key laboratory of whole-period monitoring and precise intervention of digestive cancer (SMHC)
Yu-Qin Mao
Key laboratory of whole-period monitoring and precise intervention of digestive cancer (SMHC)
Shi-Long Zhang
Key laboratory of whole-period monitoring and precise intervention of digestive cancer (SMHC)
Li-Ying Huang
The Department of Geriatrics, Ren-Ji Hospital, Shanghai Jiao-Tong University School of Medicine
Zhao-Xia Wu
Key laboratory of whole-period monitoring and precise intervention of digestive cancer (SMHC)
Hui-Ling Chen
Key laboratory of whole-period monitoring and precise intervention of digestive cancer (SMHC)
Chao-Yue Kong
Key laboratory of whole-period monitoring and precise intervention of digestive cancer (SMHC)
Zheng-Yan Zhang
Key laboratory of whole-period monitoring and precise intervention of digestive cancer (SMHC)
Zhu-Jun Yao
State Key Laboratory of Coordination Chemistry, School of Chemistry and Chemical Engineering, Nanjing University
Guoqiang Chen
Shanghai Jiao Tong University School of Medicine https://orcid.org/0000-0003-4936-2363

Biological Sciences - Article

Keywords: Obesity, HADHA, AA005

Posted Date: February 26th, 2021

DOI: https://doi.org/10.21203/rs.3.rs-228435/v1

Abstract

Obesity and related disease is a serious threat to people's health. However, currently available anti-obesity drugs couldn't fully meet the clinic needs. We found annonaceous acetogenin mimic AA005 treatment could resist obesity in diet-induced obese mice and leptin-deficient (*ob/ob*) mice at non-cytotoxic dose. Then, with a bait of biotin labeled AA005, 44 proteins were captured as AA005 binding proteins using chemical proteomics. Alpha subunit of mitochondrial trifunctional protein (HADHA) showed the strongest affinity and its knockdown suppressed the fat accumulation in 3T3-L1 cells, identical to the effect of AA005. Pharmacokinetic analysis indicated that AA005 were mainly distributed in liver and fat tissue, and thus we constructed tissue-specific HADHA knockout mice of liver and fat. The obesities induced by high fat diet in these mice were significantly inhibited. Intriguingly, elevating energy expenditure and activated thermogenesis pathway were detected in AA005-treated as well as HADHA knockout mice. Thus, AA005 targeting HADHA may serve as novel therapeutic strategy for obesity.

Background

The worldwide obesity epidemic presents a pressing public health crisis[1,2]. More than 2.1 billion individuals throughout the world are overweight or obese, and 3.4 million deaths per year are caused by obesity-related diseases[3]. Obesity is a major cause for the development of debilitating conditions such as type 2 diabetes, cardiovascular disease, hypertension, and non-alcoholic steatohepatitis, which impair life quality as well as lifespan[4,5]. Drugs that safely reverse obesity could benefit to large number of people.

Currently, only five medications approved for long-term weight management by the Food and Drug Administration (FDA), include three single drugs (orlistat, liraglutide, lorcaserin), and two combination drugs (phentermine-topiramate and naltrexone-bupropion)[6-8]. However, these five drugs can only help patients achieve moderate weight loss, and they all have multiple side effects[9-13]. Consequently, there is an urgent need to explore more safe and effective new compounds for the treatment of obesity, especially those compounds derived from or originating in nature plants.

AA005, a recently-identified new annonaceous acetogenin mimic who demonstreated selective antitumor activity *in vivo* in our previous work[14-19]. Interestingly, recent studies have shown that crude leaf extracts from *Annonaceae* plants have potential anti-diabetes and antioxidant effects, which strongly prompted us to investigate other pharmacological activities of AA005[20]. To test the effects of AA005 (Fig. 1a) on obesity, we fed mice with an HFD for 22 weeks and supplemented the animals' diet with daily administration of AA005 or vehicle as negative control. Notably, AA005 prevented HFD-induced weight gain from week 3 onwards (Fig. 1b), and these findings were not accompanied by energy intake changes (Fig. 1c), thereby excluding the toxic effect of AA005 on appetite. At the end of the 22rd week, body weight of AA005-receiving diet-induced obese (DIO) mice decreased from 53.5 ± 0.9 g to 47.6 ± 2.67 g, corresponding to a 11% weight loss relative to the vehicle-treated control DIO mice (Fig. 1b, d). Furthermore, compared with vehicle-treated control DIO mice, the body fat content of AA005-treated mice was significantly reduced (Fig. 1e). Specifically, AA005 prevented fat accretion in four fat depots,

including two subcutaneous (ie, posterior-subcutaneous WAT (psWAT) and anterior-subcutaneous WAT (asWAT)), and two visceral fat (ie, epididymal (eWAT) and retroperitoneal WAT (rWAT)) (Fig. 1f). Consistent with the phenotype, AA005-treated DIO mice were protected from increased adipocyte size (Fig. 1g). In addition, the decrease in liver weight and hepatic fat infiltration could well explain the reduction of lean mass content in the AA005-treated mice (Fig. 1h, i). Consistent with the lean phenotype, HFD-induced glucose tolerance (Fig. 1j, k), and insulin resistance (Fig. 1l, m) were significantly improved after AA005 treatment, indicating enhanced insulin sensitivity. Furthermore, we have also administered vehicle or AA005 to WT mice that were kept on chow diet (CD) for 22 weeks, and found no significant alterations after the long-term chronic administration showing that AA005 did not create toxic effect in mice (Extended Data Fig.1).

Leptin is an adipocyte-derived hormone, which is the main messenger that carries information about peripheral energy stores to the CNS[21,22]. There is a notion that obesity is a condition of leptin resistance, or leptin insensitivity[23]. In order to determine whether AA005 is a leptin sensitizer, we first detected the circulating leptin level of DIO and leptin-deficient (*ob/ob*) mice and found no significant changes for plasma leptin level after long-term treatment with AA005 (Extended Data Fig. 2a, b). To further verify this result, we next tested whether AA005 has a weight loss effect in *ob/ob* mice.

Similar to what was observed in DIO mice, administration of AA005 significantly diminished body weight gain of *ob/ob* mice by approximately 10% (Extended Data Fig. 2c, d), and also reduced their fat mass, especially the three fat depots, psWAT, asWAT and eWAT (Extended Data Fig. 2e). Although AA005 significantly reduced body fat content, but had no effect on lean mass content (Extended Data Fig. 2f). Furthermore, AA005 reduced the adipocyte volume (Extended Data Fig. 2g). Post-glucose challenge, AA005 enhanced glucose clearance (Extended Data Fig. 2h, i), whereas insulin sensitivity was improved in AA005-treated *ob/ob* mice versus vehicle control mice (Extended Data Fig. 2j, k). In addition, the weekly food intake for the control group and AA005-treated group showed no alterations either in wild-type or *ob/ob* mice, excluding AA005's anorectic effect for mice (Extended Data Fig. 2l). Taken together, these data demonstrate that the anti-obesity effect of AA005 does not depend on the action of leptin signaling pathway.

Our previous findings suggested that high dose of AA005 suppressed human colon cancer cell growth *in vivo* mediated by apoptosis-inducing factor (AIF) and mitochondrial Complex I components[15,16]. Evidence from other studies showed that muscle- and liver-specific AIF ablation in mice could counteract the development of insulin resistance, diabetes, and obesity[24]. We then tested protein levels of AIF and Complex I subunits NDUFB6 in AA005-treated DIO and *ob/ob* mice, but found no significant alteration (Extended Data Fig. 3). In order to identify the potential targets of AA005 for anti-obesity, we therefore tested the effect of AA005 on mouse 3T3-L1 cells, which were classical cell model for studying lipid metabolism[25]. When 3T3-L1 cells were induced to adipogenesis upon exposure to a mixture hormonal stimuli, Oil-Red-Ostaining on day 8 after induction showed that 300 nM AA005 reduced the accumulation of lipid droplets by approximately 90% (Fig. 2a). Furthermore, the expression levels of adipocyte markers

C/EBPa, PPARg and C/EBPb were significantly downregulated in AA005-treated cells compared to those in control cells during the adipogenesis process (Fig. 2b). The cell viability is fine after 300nM AA005 treatment for 8 days (Extended Data Fig. 4), excluding the cytotoxicity of this concentration of AA005 on 3T3-L1 cells.

Recently, chemical proteomics, which combines affinity purification using small molecule as bait and protein identification using mass spectrometry, is rapidly developed to be a powerful method for target identification[26,27]. It is promising to find novel targets by its inherent unbiased characters[28]. Synthetic derivatives of natural products have been shown to be useful chemical probes[29]. Thus, the chemical probe biotin-tagged AA005 (hereafter named biotin-AA005) was designed on the basis of structure-activity relationship information (Fig. 2c), which retained the activity to block fat accumulation in 3T3-L1 cells (Fig. 2d). Furthermore, biotin-AA005 was shown to localize in mitochondria (Fig. 2e) as demonstrated by the immunofluorescence with streptavidin-fluorescein isothiocyanate (FITC) and Mito-Tracker probe, and this result was consistent with previous reports that AA005 worked in mitochondria inside cancer cells[30]. Then, we isolated mitochondrial, nuclear and cytosolic fractions from 3T3-L1 cells, and western blotting was applied to determine the purity of the isolated subcellular fractions (Extended Data Fig. 5). Next, the 3T3-L1 cells subcellular fractions lysates were incubated with equivalent dose of biotin or biotin-AA005, and after affinity purification by beads with streptavidin, the proteins were preliminary separated by SDS-PAGE (Fig. 2f). As shown in Figure 2f, the proteins enriched by biotin-AA005 was mainly localized in mitochondria. For each biological replicate, proteins of each group were collected from an entire lane of an SDS-PAGE gel of equal size. To identify true interacting proteins of AA005 among all 3T3-L1 cells mitochondria proteins, we compared the relative level of tryptic peptides abundances from each group using label-free spectral count-based quantitation. 44 proteins were identified to be significantly enriched by biotin-AA005 (Extended Data Table 1). In order to test the affinity of proteins to biotin-AA005, six proteins with the most obvious modulations were verified by western blotting, and a subunit of mitochondrial trifunctional protein (HADHA) was shown the strongest affinity (Extended Data Fig. 6).

To determine whether HADHA has a functional role during the adipocyte differentiation, two pairs of shRNAs (shHADHA#1 and shHADHA#2) targeted specifically against *HADHA* were used to knockdown HADHA expression together with the non-specific scramble shRNA (shNC) as a negative control. shRNA but not shNC significantly silenced HADHA expression (Fig. 2g). Oil-Red-O staining on day 8 after differentiation induction showed that knockdown of HADHA in 3T3-L1 cells completely blocked the accumulation of lipid droplets compared with control cells (Fig. 2h). Furthermore, the expression levels of adipocyte markers were also downregulated in HADHA knockdown cells compared to those in NC cells (Fig. 2i). The phenotype was consistent with what seen in 3T3-L1 cells treated by AA005, suggesting HADHA was the most potential target of AA005 on fat accumulation.

To further explore the relationship between HADHA and AA005, we validated whether HADHA could bind AA005. As shown in Figure 2j, the biotin-AA005 instead of biotin could enrich HADHA after affinity purification. Furthermore, the binding of HADHA by biotin-AA005 could be competitively blocked by high

concentration of AA005, indicating that both AA005 and biotin-AA005 bind the same site of HADHA. Furthermore, we introduced microscale thermophoresis (MST) as a tool to characterize protein and small-molecule interactions in complex biological liquids[31], gathering information on binding under conditions close to *in vivo* situation. pFLAG-CMV4 and pFLAG-CMV4-HADHA were transfected into human embryonic kidney cells (HEK-293 cells) respectively (Extended Data Fig. 7). With MST, AA005 interactions can be quantified in cell lysate. The AA005 titration series in the HEK-293 cell lysate were performed and the affinity constant Kd values for the HADHA to AA005 was determined to about 2.57 μM (Extended Data Fig. 8). These results support that HADHA binds AA005, potentially participates in lipid accumulation.

In order to determine that HADHA is the endogenous target of AA005 against obesity, we next analyzed the dynamic tissue distribution of AA005 in mice. Intriguingly, pharmacokinetic analysis indicated that AA005 was widely distributed throughout all tissues, but most of them were located in liver and fat (Fig. 3a). Then we generated the conditional deletion of HADHA in mice using CRISPR-Cas9 system. Crossing the conditional HADHA mice to those bearing a transgene for cre-recombinase under control of either the liver albumin promoter (Alb-*cre*) or the fat fabp4 promoter (Fabp4-*cre*), we generated mice displaying liver- or fat- specific HADHA deficiencies (*HADHA*$^{flox/flox}$; Alb-*cre*/+ and *HADHA*$^{flox/flox}$; Fabp4-*cre*/+ respectively) (Extended Data Fig. 9a and 11a). Both LHADHAKO (liver-specific HADHA knockout) and FHADHAKO (fat-specific HADHA knockout) pups were born healthy, viable, and at normal Mendelian ratios. Western blotting confirmed efficient deletion of the HADHA allele specifically in the liver in LHADHAKO animals (Extended Data Fig. 9b). Morphological, histological, and blood glucose analyses to assess liver and fat condition revealed no abnormalities after 18 weeks in either set of mice fed CD (Extended Data Fig. 10 and 11).

We next examined whether liver-specific loss of HADHA would render mice resistant to obesity. As expected, LHADHAKO mice showed a marked resistance to HFD-induced body weight gain, which confirmed the strong effects of HADHA ablation on weight loss (Fig. 3c-e). Measurement of fat pad weights confirmed marked adipose deposition in control animals after high-fat feeding, but with little discernable impact on the knockout animals, especially in the five fat depots, psWAT, asWAT, pgWAT, rWAT and mesenteric white adipose tissues (mWAT) (Fig. 3c-e). On the other hand, high-fat diet-induced hepatic steatosis were almost completely prevented in LHADHAKO mice (Extended Data Fig. 9c, d). Notably, LHADHAKO mice showed improved glucose tolerance (Fig. 3f, Extended Data Fig. 9e), and insulin sensitivity (Fig. 3g, Extended Data Fig. 9f). The balance between food intake and energy expenditure determines body weight and adiposity. The reduced adiposity of LHADHAKO mice was not due to decreased food intake (Fig. 3h), or increased physical activity (Fig. 3i, Extended Data Fig. 9g) and suggested potent energy expenditure in LHADHAKO mice. As expected, energy expenditure was greatly elevated in LHADHAKO mice (Fig. 3j, k, Extended Data Fig. 9h), which was confirmed by increased O_2 consumption (Fig. 3l, m) and CO_2 production (Fig. 3n, o). We compared body weight changes of wild-type and LHADHAKO mice fed chow diet (CD), and found that LHADHAKO mice exhibited slightly reduced weight compared to wild type controls (Extended Data Fig. 10a-d). Finally, we did not observe any

significant differences in life activities between LHADHAKO and wild-type mice, which ruled out the toxicity of liver-specific loss of HADHA to mice (Extended Data Fig. 10e-t). Similar weight-loss effect were obtained in FHADHAKO mice (Extended Data Fig. 11). Together, these data demonstrate that ablation of HADHA in fat or liver tissue specifically protects mice from obesity mostly by elevating energy expenditure.

To obtain an unbiased understanding of the underlying molecular mechanism of anti-obesity effect in LHADHAKO mice, we performed RNA-seq analysis using fresh residual psWAT of AA005-receiving DIO mice, high-fat diet fed LHADHAKO mice as well as the untreated control mice. Comparison of the control groups, 2030 up-regulated RNA species were identified in AA005 group, and 305 in LHADHAKO group, of which 146 were consistent with the AA005 group, and the proportion of down-regulated RNAs in the two groups was greater (Fig. 4a). Interestingly, our analysis revealed that the gene expression profiles of AA005-treated DIO mice and high-fat fed LHADHAKO mice were highly similar (Fig. 4b). Differentially expressed genes and transcripts were determined for further analysis. Biological function analysis for all differentially expressed genes revealed that Kyoto Encyclopedia of Genes and Genome (KEGG) terms associated with “metabolic process” were notably actived (Fig. 4c). The heatmap showed that AA005 treatment and HADHA deficiency mainly upregulated the protein processing in thermogenesis signaling pathway, and downregulated other pathways such as adipogenesis regulation, fatty acid metabolism, and cholesterol metabolism (Fig. 4d). Consistent with the strong upregulation of thermogenesis associated genes in AA005-receiving DIO mice and high-fat fed LHADHAKO mice, HADHA were found to be central nodes in the network interacted with UCP1, UCP2 and UCP3 (Fig. 4e). To validate the RNA-seq results, we tested the mRNA levels of the specific marker genes involved in thermogenesis pathway using real-time RT-PCR. The results showed that AA005 treatment and HADHA deficiency did activate the thermogenesis pathway (Fig. 4f, g), which might explain the pharmacological effects of AA005 regulating HADHA against obesity.

Obesity is a complex disorder that is difficult to overcome. Mitochondrial uncoupling can cause weight loss without affecting foodintake. Recent years have seen a resurgence of interest in mitochondrial uncouplers as human medicines[32]. For example, niclosamide has been reported in a diet-induced obesity prevention model where its lowed not only fat mass gain but also diminished lean mass gain[33]. In contrast to niclosamide, AA005 treatment in the obese mice decreased fat mass without decreasing lean mass (except fatty liver) thereby revealing are markably high specificity for AA005 to target fat loss. So, the preservation of lean mass during weight loss is highly desired and distinguishes AA005 from other uncouplers. OPC-163493, as a mitochondrial uncoupler, recently discovered had strong anti-diabetes effects in multiple rodent models, but did not impact adiposity[34]. Our work have shown that AA005 improved glucose tolerance and insulin sensitivity in obese mice suggesting its potential antidiabetic effects.

The previous studies have reported that the hetero eight polymer complex composed of HADHA and b subunit of mitochondrial trifunctional protein (HADHB) plays a role in the catalysis of mitochondrial long chain fatty acids oxidation[35]. Furthermore, the mice with HADHA homozygote deletion were born light

weight and appeared neonatal hypoglycemia and sudden death within 6-36 hours after birth[36]. This phenomenon could not be explained by the known functions of HADHA, suggesting that HADHA is likely to perform new biological functions in lipid metabolism, which is worthy of further study. Here, using HADHA-conditional mutant mice, we verified that the mice could resist obesity and metabolic disease, implying a novel role for HADHA in regulating lipid metabolism.

In summary, AA005 represents a new type of anti-obesity compound, which is characterized by specifically targeting HADHA to increase energy expenditure without affecting food intake or lean mass. One limitation of AA005 is low aqueous solubility, but this property did not affect oral bioavailability and indeed low aqueous solubility is an important parameter that enables AA005 to penetrate membranes and enter mitochondria. Collectively, the data presented herein supports further development of AA005 as a potential therapeutic for obesity and metabolic diseases.

Methods

Chemicals and reagents. Annonaceous acetogenin mimic AA005 (kindly supplied by the State Key Laboratory of Coordination Chemistry, Nanjing University, Nanjing, China) was dissolved in dimethylsulfoxide as a 5 mM stock solution and was stored at −80 °C. Antibodies against AIF (#4642), PPARg (#2443), C/EBPb (#3087), Lamin B1 (#12586), Cox IV (#4844), and β-actin (#3700) were purchased from Cell Signaling Technology (Beverly, MA, USA), NDUFB6 (16037-1-AP) and HADHA (#ab203114) were purchased from Proteintech Group, mouse C/EBPa (sc-61) were from Santa Cruz Biotech.

Animal procedures and ethics statement. Animal experiments were performed according to procedures approved by the Institutional Animal Care and Use Committee of Key laboratory of whole-period monitoring and precise intervention of digestive cancer (SMHC). All mice used in this study were on C57BL/6 background and housed in a specific pathogen-free (SPF) facility on a 12 h light/dark cycle. To generate a HADHA knockout mouse line by CRISPR-Cas9 genome editing system, a single-guide RNA (sgRNA) was designed to target the exon 3 of the HADHA gene locus. Crossing the conditional line to mice expressing *Cre*-recombinase under control of the Albumin or fabp4 promoter yielded the liver-specific or fat-specific AIF knockout mice.

Glucose and insulin tolerance Test. The animals were fasted overnight, blood was collected from the tail vein to measure fasting plasma glucose, and then 2 g glucose per kilogram of body weight was injected intraperitoneal. Blood was collected 15, 30, 60, 90, and 120 minutes after glucose injection, and blood glucose was measured by a blood glucose meter (Ascensia, Contour, Bayer Healthcare, Oslo, Norway). Subsequently, an insulin tolerance test was performed. The animals were fasted for 6 hours, blood was collected from the tail vein to measure fasting blood glucose, and then 0.75 U insulin per kilogram of body weight was injected intraperitoneally (Actrapid, Novo Nordisk, Bagsværd, Denmark). Blood was collected 15, 30, 60, 90 and 120 minutes after the insulin injection, and blood glucose was measured by a blood glucose meter.

Immunohistochemical staining. Immunohistochemical (IHC) staining was applied to detect the protein levels of AIF and NDUFB6 in vehicle or AA005-treated mice fed CD or HFD with anti-AIF (#4642, Cell Signaling Technology, Danvers, MA, USA) or anti-NDUFB6 (16037-1-AP, Proteintech Group, Chicago, IL) antibodies. IHC staining was performed according to the manufacturer's protocol.

Cell culture and induction of adipogenesis. 3T3-L1 preadipocytes were grown and maintained in DMEM containing 10% (vol/vol) calf serum. Two-day postconfluent (designated as day 0) cells were induced to differentiate with DMEM containing 10% (vol/vol) fetal bovine serum (FBS), 1 mg/ml insulin (I), 1 mM dexamethasone (DEX), and 0.5 mM 3-isobutyl-1-methylxanthine (MIX) until day 2. Cells were fed with DMEM supplemented with 10% FBS and 1ug/ml insulin for 2 days, followed every two days changing with DMEM containing 10% FBS. At the times indicated (day 8), cells were stained with Oil Red O to detect cytoplasmic triglyceride, extracted and immunoblotted.

Immunofluorescence. 3T3-L1 cells were crawled onto cover slides. After treated with 10 mM biotin-AA005 for 4 hours, 3T3-L1 cells were incubated in the mitochondrial probe mito-tracker (1 mM)-containing medium for 30 minutes. Then, cells were fixed with 4% paraformaldehyde and permeabilized with 0.3% Triton X-100 for 10 min. Slides were blocked with 1% bovine serum albumin and incubated with streptavidin-FITC (1:100) overnight at 4°C. After washing in PBS, the cells were stained with nuclear counterstaining DAPI. Fluorescence signals were detected on a Olympus BX-51 fluorescence microscope (Tokyo, Japan).

Subcellular cell fractionation and mitochondria purification. Cells were separated into different fractions according to previously described methods[37,38]. In brief, cells were harvested and rinsed with mitochondria isolation buffer (MIB, 0.25 M sucrose and 10 mM Tris-HCl, pH 7.4), resuspended in MIB supplemented with 1% protease inhibitor cocktail and homogenized using a glass Dounce homogenizer (Kontes, Sigma-Aldrich) with 20 strokes at 4 °C. The homogenate was centrifuged at 1,000 g for 10 min to pellet the nucleus. The supernatant was centrifuged at 15,000 g for 20 min at 4 °C to pellet the raw mitochondria. Cytoplasmic proteins in the post-mitochondria supernatant were precipitated with chloroform and methanol according to Klotz's methods[39]. To further enrich the mitochondria, the pellet of raw mitochondria was resuspended in 36% iodixanol (Sigma-Aldrich) and overlaid with 30% and 10% iodixanol. The gradient was ultracentrifuged (80,000 *g*, 3 h) at 4 °C. The purified mitochondria were collected at the interface between 10% and 30% iodixanol and washed twice with MIB. Samples of each fraction were prepared by addition of sample buffer and subjected to immunoblot analysis.

Western blots. Cells were rinsed with ice-cold 1×PBS and lysed in nonreducing buffer containing 100 mM Tris–HCl, pH 6.8, 2% SDS, 50 mM IAA, supplemented with PMSF and cocktail, or reducing buffer containing an additional 100 mM DTT. Cell lysates were separated on a 8–12.5% SDS-polyacrylamide gel, transferred to a nitrocellulose membrane (Bio-Rad, Richmond, CA), blocked with 5% nonfat milk in PBS, and immunoblotted with the indicated antibodies. After incubation with the horseradish peroxidase-linked second antibody (Cell Signaling, Beverly, MA, USA) at room temperature, detection was performed

using the SuperSignal West Pico Chemiluminescent Substrate Kit (Pierce, Rockford, IL) according to the manufacturer's instructions.

Oil Red O staining and quantifying. Cells were washed three times with PBS and fixed for 10 min with 3.7% formaldehyde. Oil Red O (0.5% in isopropanol) was diluted with water (3:2), filtered through a 0.45 mm filter. Cells were stained for 3~4 h at room temperature, washed three times with water, and stained fat droplets in the cells were examined by light microscopy and photographed. After photographed, Oil Red O was eluted by adding 100% isopropanol and incubated 10 min at room temperature. Then transfer to 1 ml solution to cuvette and measure OD at 520nm in spectrophotometer.

Pull-down and MS analysis of AA005-bound proteins. The mitochondria was isolated from 3T3-L1 cells, and the mitochondrial fractions lysates were incubated with biotin or biotin-AA005 overnight at 4 °C, followed by pull-down with streptavidin-agarose beads, and the bead-bound proteins were separated by SDS-PAGE and visualized by Coomassie blue staining. The protein-containing band in the gel was excised, followed by in-gel digestion and analysis by LC-MS/MS. Pull-down and MS analysis was performed, and the data were analyzed according to our previous report[26,27].

Tissue Distribution Study. To investigate the tissue distribution characteristics of AA005 in mice, C57BL/6 mice (n=3) were given a single oral dose of 17 mg/kg AA005. After 0.25, 1, 2, and 6 h, all tissues, including the plasma, liver, heart, pancreas, kidney, lung, fat, spleen, brain, testis, stomach, and intestine were separated and homogenized, and their AA005 concentrations were detected by UPLC-MS/MS.

RNA-sequencing. Posterior-subcutaneous white adipose tissue (psWAT) of mice were collected with Trizol reagent. The total RNA was processed by NEBNext®Poly(A) mRNA Magnetic Isolation Module to enrich mRNA, and the product RNA was used for construction Library, via KAPA Stranded RNA-Seq Library Prep Kit (Illumina). Sequencing libraries, denatured by 0.1M NaOH to generate single-stranded DNA, as amplified in situ Illumina cBot (TruSeq SR Cluster Kit v3-cBot-HS (#GD-401-3001, Illumina)). The ends of the generated fragments were used to run 150 Cycles by the Illumina HiSeq 4000 Sequencer. All the experimental steps after the RNA extraction were conducted in Kangcheng Biotechnology Co., Ltd. (Aksomics), Shanghai, China. RNA-sequencing was performed three times.

Real-time quantitative RT-PCR. Total RNA from the cell lines were extracted with TRIzol reagent (Invitrogen, Carlsbad, CA) and treated with RNase-free DNase (Promega, Madison, WI, USA). Quantitative real-time PCR was performed using the SYBR Green PCR Master Mix (Applied Biosystems, Foster City, CA, USA). The primers used are listed as follows: UCP1-5'- AGGCTTCCAGTACCATTAGGT-3'(forward), 5'-CTGAGTGAGGCAAAGCTGATTT-3'(reverse), UCP2-5'-ATGGTT

GGTTTCAAGGCCACA-3'(forward), UCP2-5'-TTGGCGGTATCCAGAGGGAA-3'(reverse), PGC-1a-5'-AGCCGTGACCACTGACAACGAG-3' (forward), PGC-1a-5'- GCTGCATGGTTCTGAGTGCTAAG-3'(reverse), PGC-1b-5'- TCCTGTAAAA

GCCCGGAGTAT-3'(forward), PGC-1b-5'- GCTCTGGTAGGGGCAGTGA-3'(re-verse), Cidea-5'-TGCTCTTCTGTATCGCCCAGT-3' (forward), Cidea -5'-GCCGT

GTTAAGGAATCTGCTG-3'(reverse), Tfam-5'-GGAATGTGGAGCGTGCTAAAA-3' (forward), Tfam -5'-ACAAGACTGATAGACGAGGGG-3'(reverse), with b-actin-5'-CATCCTCACCCTGAAGTACCC-3' (forward), 5'-AGCCTGGATAGCAACGTA

CATG-3'(reverse). Real-time RT-PCR was performed, and the data were analyzed according to a previous report[40].

Statistical analysis. Each experiment was done independently at least 3 times with similar results. Results are expressed as mean ± S.D. Significant differences were assessed with the Student's *t* test (2-tailed). $p < 0.05$ was considered to be significant. For *in vivo* studies, mice were randomly assigned to treatment groups. Mass spectrometric analyses were blinded to experimental conditions

Declarations

Acknowledgments This work was financially supported by the National Natural Science Foundation of China (81803601, 81872245). This work is supported in part by grants from Shanghai Sailing Program (Grant No. 17YF1416700).

Author contributions BH and LSW conceived and designed the experiments; BH, ZML, YQM, SLZ, LYH, ZXW, HLC, CYK, and ZYZ performed the experiments; BH, ZJY, GQC and LSW analyzed the data; BH and LSW wrote the paper. All authors read and approved the final manuscript.

Competing financial interests The authors declare that they have no competing financial interests.

Reference

1 Finucane, M. M. *et al.* National, regional, and global trends in body-mass index since 1980: systematic analysis of health examination surveys and epidemiological studies with 960 country-years and 9.1 million participants. *Lancet***377**, 557-567, doi:10.1016/S0140-6736(10)62037-5 (2011).

2 Swinburn, B. A. *et al.* The global obesity pandemic: shaped by global drivers and local environments. *Lancet***378**, 804-814, doi:10.1016/S0140-6736(11)60813-1 (2011).

3 Ng, M. *et al.* Global, regional, and national prevalence of overweight and obesity in children and adults during 1980-2013: a systematic analysis for the Global Burden of Disease Study 2013. *Lancet***384**, 766-781, doi:10.1016/S0140-6736(14)60460-8 (2014).

4 Olshansky, S. J. *et al.* A potential decline in life expectancy in the United States in the 21st century. *N Engl J Med***352**, 1138-1145, doi:10.1056/NEJMsr043743 (2005).

5 Lauby-Secretan, B. *et al.* Body Fatness and Cancer–Viewpoint of the IARC Working Group. *N Engl J Med***375**, 794-798, doi:10.1056/NEJMsr1606602 (2016).

6 Heymsfield, S. B. & Wadden, T. A. Mechanisms, Pathophysiology, and Management of Obesity. *N Engl J Med***376**, 1492, doi:10.1056/NEJMc1701944 (2017).

7 Yanovski, S. Z. & Yanovski, J. A. Long-term drug treatment for obesity: a systematic and clinical review. *JAMA***311**, 74-86, doi:10.1001/jama.2013.281361 (2014).

8 Apovian, C. M. *et al.* Pharmacological management of obesity: an endocrine Society clinical practice guideline. *J Clin Endocrinol Metab***100**, 342-362, doi:10.1210/jc.2014-3415 (2015).

9 Davidson, M. H. *et al.* Weight control and risk factor reduction in obese subjects treated for 2 years with orlistat: a randomized controlled trial. *JAMA***281**, 235-242, doi:10.1001/jama.281.3.235 (1999).

10 Pi-Sunyer, X. *et al.* A Randomized, Controlled Trial of 3.0 mg of Liraglutide in Weight Management. *N Engl J Med***373**, 11-22, doi:10.1056/NEJMoa1411892 (2015).

11 Smith, S. R. *et al.* Multicenter, placebo-controlled trial of lorcaserin for weight management. *N Engl J Med***363**, 245-256, doi:10.1056/NEJMoa0909809 (2010).

12 Gadde, K. M. *et al.* Effects of low-dose, controlled-release, phentermine plus topiramate combination on weight and associated comorbidities in overweight and obese adults (CONQUER): a randomised, placebo-controlled, phase 3 trial. *Lancet***377**, 1341-1352, doi:10.1016/S0140-6736(11)60205-5 (2011).

13 Apovian, C. M. *et al.* A randomized, phase 3 trial of naltrexone SR/bupropion SR on weight and obesity-related risk factors (COR-II). *Obesity (Silver Spring)***21**, 935-943, doi:10.1002/oby.20309 (2013).

14 Zeng, B. B. *et al.* Studies on mimicry of naturally occurring annonaceous acetogenins: non-THF analogues leading to remarkable selective cytotoxicity against human tumor cells. *Chemistry***9**, 282-290, doi:10.1002/chem.200390021 (2003).

15 Han, B. *et al.* Annonaceous acetogenin mimic AA005 suppresses human colon cancer cell growth in vivo through downregulation of Mcl-1. *Acta Pharmacol Sin***40**, 231-242, doi:10.1038/s41401-018-0025-7 (2019).

16 Han, B. *et al.* Annonaceous acetogenin mimic AA005 induces cancer cell death via apoptosis inducing factor through a caspase-3-independent mechanism. *BMC Cancer***15**, 139, doi:10.1186/s12885-015-1133-0 (2015).

17 Liu, H. X., Huang, G. R., Zhang, H. M., Wu, J. R. & Yao, Z. J. Annonaceous acetogenin mimics bearing a terminal lactam and their cytotoxicity against cancer cells. *Bioorg Med Chem Lett***17**, 3426-3430, doi:10.1016/j.bmcl.2007.03.084 (2007).

18 Jiang, S. *et al.* Parallel fragment assembly strategy towards multiple-ether mimicry of anticancer annonaceous acetogenins. *Angew Chem Int Ed Engl* **43**, 329-334, doi:10.1002/anie.200352681 (2004).

19 Huang, G. R. *et al.* Induction of cell death of gastric cancer cells by a modified compound of the annonaceous acetogenin family. *Chembiochem* **4**, 1216-1221, doi:10.1002/cbic.200300677 (2003).

20 Florence, N. T. *et al.* Antidiabetic and antioxidant effects of Annona muricata (Annonaceae), aqueous extract on streptozotocin-induced diabetic rats. *J Ethnopharmacol* **151**, 784-790, doi:10.1016/j.jep.2013.09.021 (2014).

21 Dietrich, M. O. & Horvath, T. L. Hypothalamic control of energy balance: insights into the role of synaptic plasticity. *Trends Neurosci* **36**, 65-73, doi:10.1016/j.tins.2012.12.005 (2013).

22 Halaas, J. L. *et al.* Physiological response to long-term peripheral and central leptin infusion in lean and obese mice. *Proc Natl Acad Sci U S A* **94**, 8878-8883, doi:10.1073/pnas.94.16.8878 (1997).

23 Considine, R. V. *et al.* Serum immunoreactive-leptin concentrations in normal-weight and obese humans. *N Engl J Med* **334**, 292-295, doi:10.1056/NEJM199602013340503 (1996).

24 Pospisilik, J. A. *et al.* Targeted deletion of AIF decreases mitochondrial oxidative phosphorylation and protects from obesity and diabetes. *Cell* **131**, 476-491, doi:10.1016/j.cell.2007.08.047 (2007).

25 Shen, S. M. *et al.* Apoptosis-inducing factor is a target gene of C/EBPalpha and participates in adipocyte differentiation. *FEBS Lett* **585**, 2307-2312, doi:10.1016/j.febslet.2011.05.061 (2011).

26 Liu, C. X. *et al.* Adenanthin targets peroxiredoxin I and II to induce differentiation of leukemic cells. *Nat Chem Biol* **8**, 486-493, doi:10.1038/nchembio.935 (2012).

27 Gao, Y. H. *et al.* VHL deficiency augments anthracycline sensitivity of clear cell renal cell carcinomas by down-regulating ALDH2. *Nat Commun* **8**, 15337, doi:10.1038/ncomms15337 (2017).

28 Schenone, M., Dancik, V., Wagner, B. K. & Clemons, P. A. Target identification and mechanism of action in chemical biology and drug discovery. *Nat Chem Biol* **9**, 232-240, doi:10.1038/nchembio.1199 (2013).

29 Kotake, Y. *et al.* Splicing factor SF3b as a target of the antitumor natural product pladienolide. *Nat Chem Biol* **3**, 570-575, doi:10.1038/nchembio.2007.16 (2007).

30 Liu, H. X. *et al.* A structure-activity guided strategy for fluorescent labeling of annonaceous acetogenin mimetics and their application in cell biology. *Chembiochem* **8**, 172-177, doi:10.1002/cbic.200600411 (2007).

31 Wienken, C. J., Baaske, P., Rothbauer, U., Braun, D. & Duhr, S. Protein-binding assays in biological liquids using microscale thermophoresis. *Nat Commun* **1**, 100, doi:10.1038/ncomms1093 (2010).

32 Geisler, J. G. 2,4 Dinitrophenol as Medicine. *Cells***8**, doi:10.3390/cells8030280 (2019).

33 Tao, H., Zhang, Y., Zeng, X., Shulman, G. I. & Jin, S. Niclosamide ethanolamine-induced mild mitochondrial uncoupling improves diabetic symptoms in mice. *Nat Med***20**, 1263-1269, doi:10.1038/nm.3699 (2014).

34 Kanemoto, N. *et al.* Antidiabetic and cardiovascular beneficial effects of a liver-localized mitochondrial uncoupler. *Nat Commun***10**, 2172, doi:10.1038/s41467-019-09911-6 (2019).

35 Ishikawa, M., Tsuchiya, D., Oyama, T., Tsunaka, Y. & Morikawa, K. Structural basis for channelling mechanism of a fatty acid beta-oxidation multienzyme complex. *EMBO J***23**, 2745-2754, doi:10.1038/sj.emboj.7600298 (2004).

36 Ibdah, J. A. *et al.* Lack of mitochondrial trifunctional protein in mice causes neonatal hypoglycemia and sudden death. *J Clin Invest***107**, 1403-1409, doi:10.1172/JCI12590 (2001).

37 Yu, Y. *et al.* Subcellular proteome analysis of camptothecin analogue NSC606985-treated acute myeloid leukemic cells. *J Proteome Res***6**, 3808-3818, doi:10.1021/pr0700100 (2007).

38 Morand, J. P., Macri, J. & Adeli, K. Proteomic profiling of hepatic endoplasmic reticulum-associated proteins in an animal model of insulin resistance and metabolic dyslipidemia. *J Biol Chem***280**, 17626-17633, doi:10.1074/jbc.M413343200 (2005).

39 Klotz, A. V., Stegeman, J. J. & Walsh, C. An alternative 7-ethoxyresorufin O-deethylase activity assay: a continuous visible spectrophotometric method for measurement of cytochrome P-450 monooxygenase activity. *Anal Biochem***140**, 138-145, doi:10.1016/0003-2697(84)90144-1 (1984).

40 Zhao, K. W. *et al.* Protein kinase Cdelta mediates retinoic acid and phorbol myristate acetate-induced phospholipid scramblase 1 gene expression: its role in leukemic cell differentiation. *Blood***104**, 3731-3738, doi:10.1182/blood-2004-04-1630 (2004).

Figures

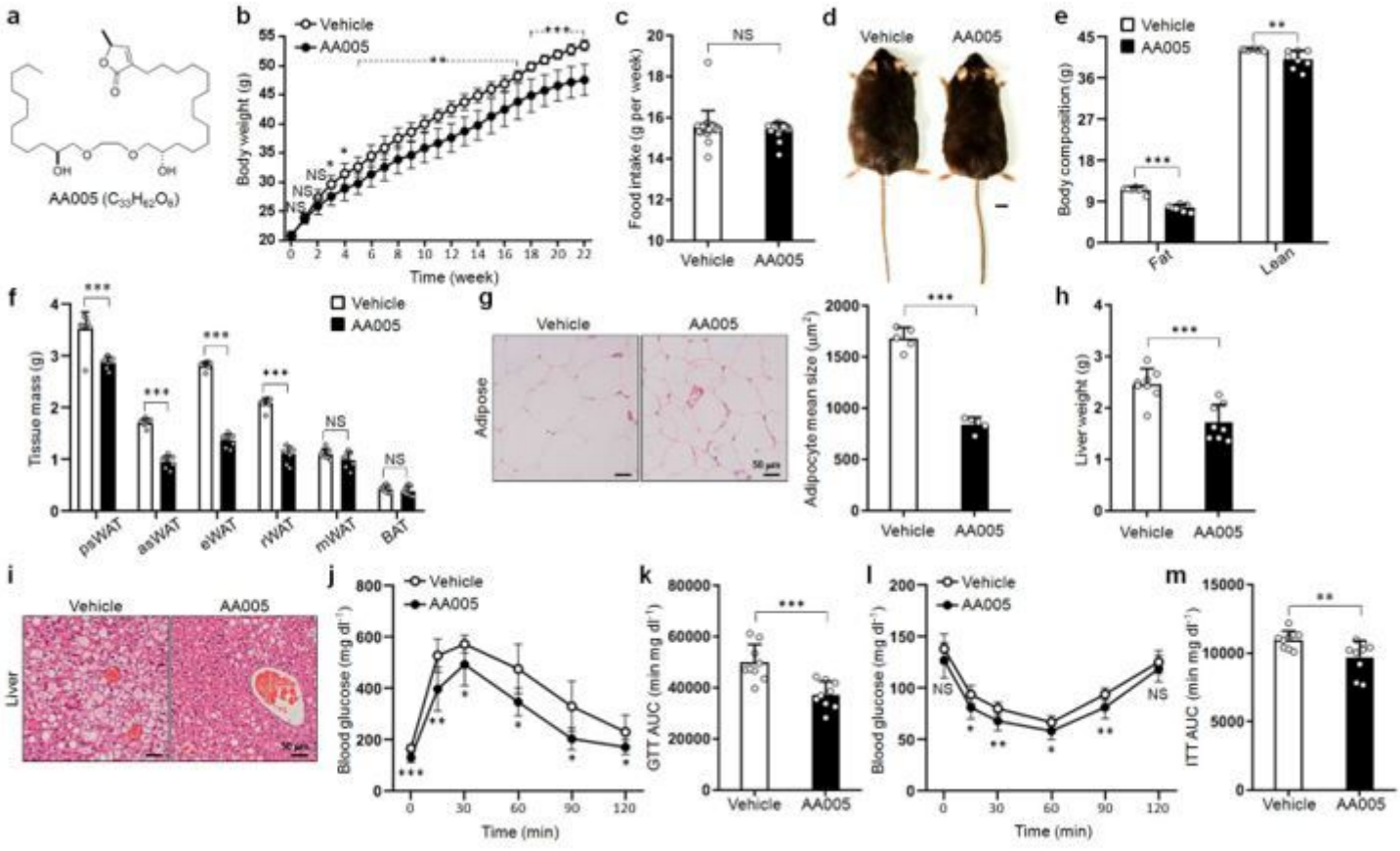

Figure 1

AA005 resists obesity and its metabolic consequences in diet-induced obese mice. a, Chemical structure of AA005. b, Weight gain of male littermates fed HFD without or with AA005 (12mg/kg contained in HFD) was recorded for 22 weeks (n=8-9 for each group). c, The average food intake of each mouse for 1 week was recorded (n=22). d, A representative photograph of 7-month-old vehicle and AA005-treated DIO mice. Scale bar, 1 cm. e, Fat and lean mass were recorded after 22 weeks treatment (n=8). f, Fat weight of psWAT, asWAT, eWAT, rWAT, mWAT and BAT in vehicle and AA005-treated DIO mice (n=8). g, Representative images of haematoxylin and eosin (H&E) stained of white adipose tissue. Image J software was used to quantify the adipocyte size (n=5). h, Weights of liver in vehicle and AA005-treated DIO mice (n=8). i, Representative images of H&E-stained liver tissues. j-m, Glucose tolerance test (GTT) (j), area under the curve (AUC) of GTT (k), insulin tolerance test (ITT) (l) and AUC of ITT (m) in vehicle and AA005-treated DIO mice (n=9). Data are mean ± S.D. *P□0.05, **P□0.01, ***P□0.001, NS means not significant.

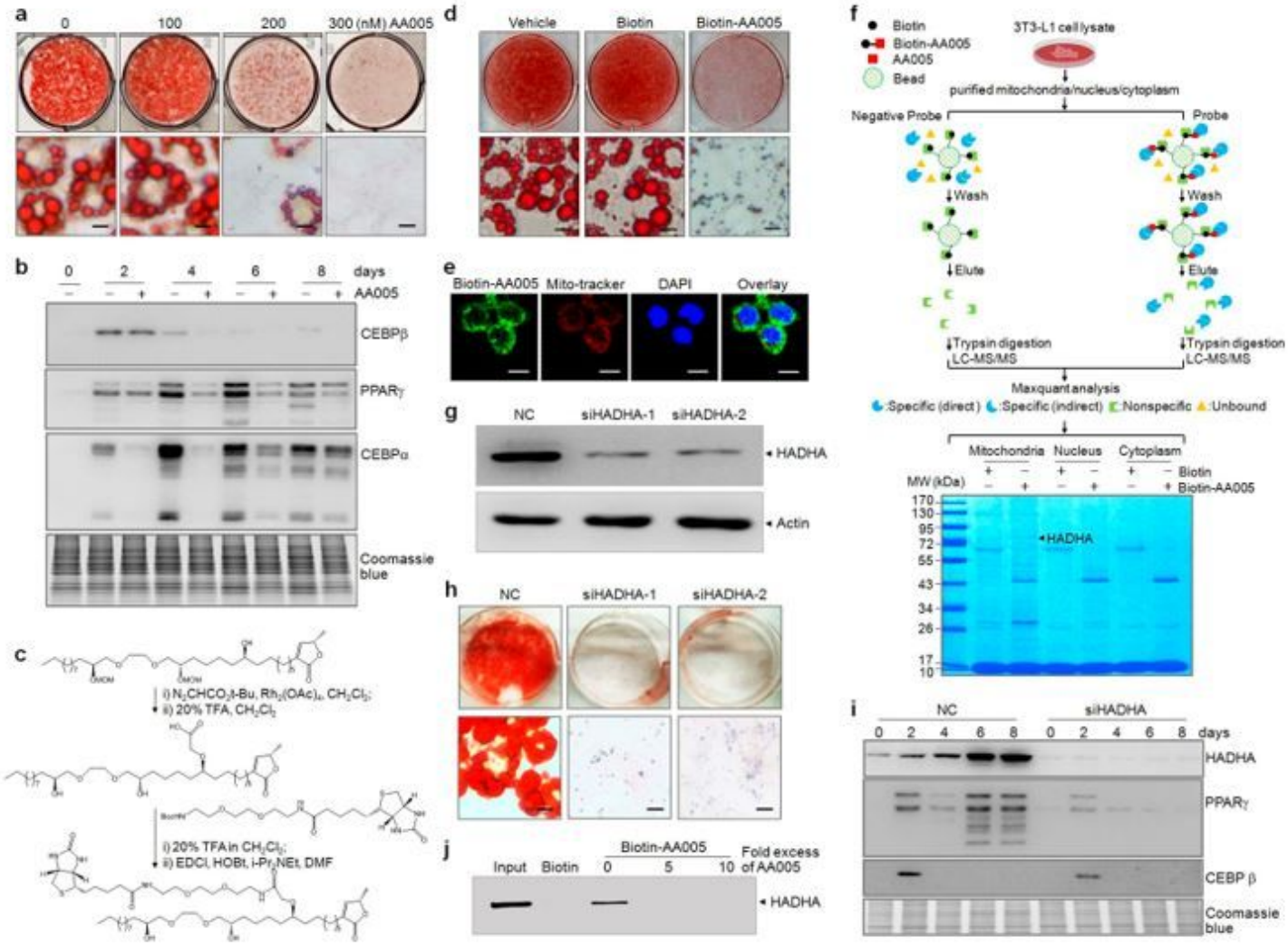

Figure 2

Mitochondrial trifunctional enzyme a subunit (HADHA) is the target of AA005. a, On day 8 after induction of adipogenesis concomitant treatment with AA005 at different concentrations, preadipocyte 3T3-L1 cells were stained with Oil-Red-O. Scale bar, 10 μm. b, After induction of adipogenesis concomitant treatment with 300 nM AA005, total protein at indicated time points were subjected to western blot with indicated antibodies. Coomassie blue staining was used as loading control. c, The workflow of biotin-tagged AA005 was shown. d, On day 8 after induction of adipogenesis concomitant treatment with biotin or biotin-AA005, 3T3-L1 cells were stained with Oil-Red-O. Scale bar, 10 μm. e, Immunofluorescence detected the location of biotin-AA005 in cells, Mito-tracter labeled mitochondria, and DAPI labeled nuclei. Scale bar, 20 m. f, A sketch of discovery interacting proteins of AA005 by chemical proteomics. g, 3T3-L1 cells which transfected with scrambled negative control (NC) or siRNAs against HADHA were harvested, and cell lysates were blotted for proteins as indicated. h, On day 8 after induction of adipogenesis, 3T3-L1-NC or 3T3-L1-siHADHA cells were stained with Oil-Red-O. Scale bar, 10 μm. i, After induction of adipogenesis, total protein at indicated time points were subjected to western blot with indicated antibodies. Standardized to coomassie blue staining. j, 3T3-L1 cell mitochondrial fractions lysates were incubated

with biotin or biotin-AA005 in the absence or presence of a 5- or 10-fold excess of unlabeled AA005, followed by pull-down with streptavidin-agarose. The precipitates were detected by western blotting for HADHA.

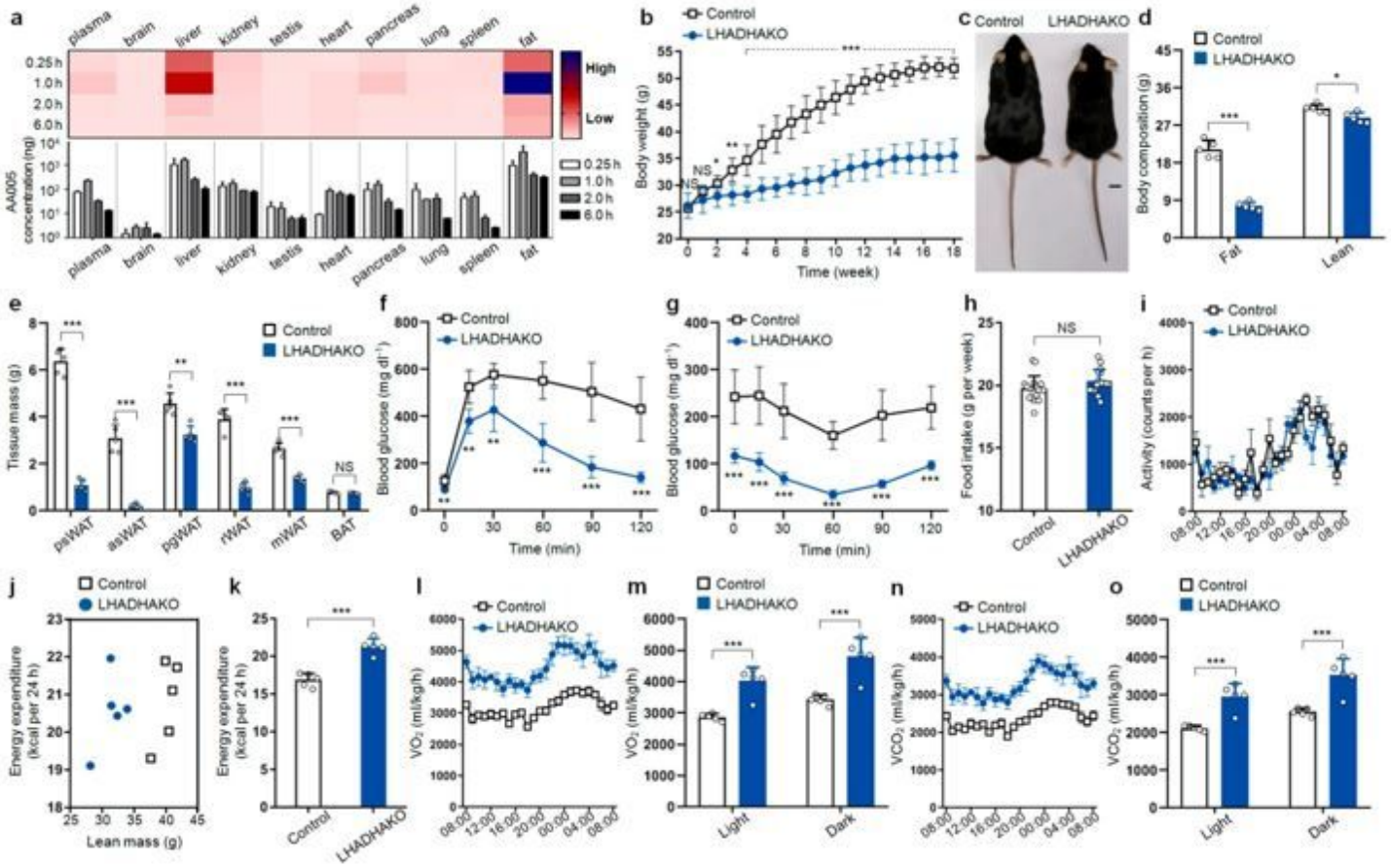

Figure 3

LHADHAKO mice are resistant to diet-induced obesity. a, The heatmap and histogram showed the tissue distributions of AA005 in mice at indicated times after single oral administration of 17 mg/kg AA005. b, Weight gain of male littermates fed HFD in control and LHADHAKO (liver-specific HADHA knockout) mice was recorded for 18 weeks (n=7). c, A representative photograph of 6-month-old control and LHADHAKO mice fed HFD. Scale bar, 1 cm. d, Fat and lean mass were recorded after 18 weeks treatment (n=5). e, Fat weight of psWAT, asWAT, eWAT, rWAT, mWAT and BAT in control and LHADHAKO mice fed HFD (n=5). f-g, Glucose tolerance test (GTT) (f), and insulin tolerance test (ITT) (g) in control and LHADHAKO mice fed HFD (n=6-7 for each group). h, The average food intake of each mouse for 1 week was recorded (n=17). i, Physical activity of male littermates fed HFD in control and LHADHAKO for a 24h recording period (n=5). j, k, 24h energy expenditure was compared between control and LHADHAKO mice. Energy expenditure per mouse was plotted against lean mass (j). The means of energy expenditure in the two groups adjusted with lean mass (k) (n=5) . l-o, O2 consumption (l, m) and CO2 production (n, o) were recorded during a 24 h period. 24 h period (l, n). Average of light and dark period, respectively (m, o) (n=5). Data are mean ± S.D. *P□0.05, **P□0.01, ***P□0.001, NS means not significant.

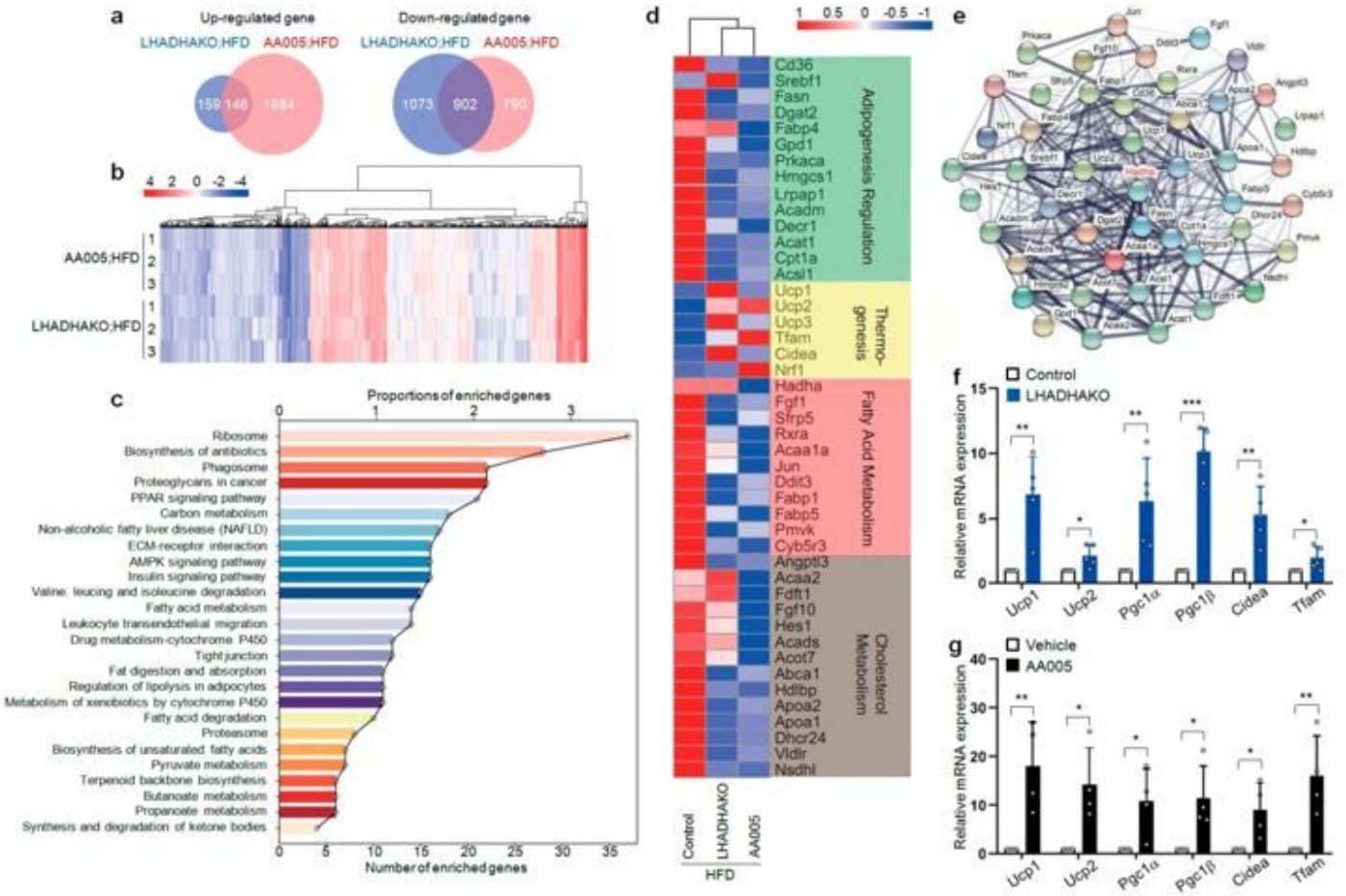

Figure 4

AA005 potentiates thermogenic pathway through HADHA. a, Difference analysis in RNA-seq of the AA005-treated and LHADHAKO mice compared to control mice fed HFD (n=3). Overlap in gene expression profiles between the two group. b, Heatmap displayed differentially regulated genes between AA005-treated and LHADHAKO mice fed HFD in psWAT (n=3). Red and blue colors indicated up-regulated or down-regulated genes. c, Significant enrichment in KEGG terms. Bars showed the number or proportions of genes within each functional class, ranked based on the protein coverage. d, Heatmap of mean fold-change of the indicated metabolic process in control, AA005-treated and LHADHAKO mice fed HFD. Red and blue colors indicated upregulated or downregulated genes. e, The interacting network of the genes regulated by both AA005 and HADHA. f, Relative mRNA levels of thermogenic genes in psWAT of control and LHADHAKO mice fed HFD (n=5). g, Relative mRNA levels of thermogenic genes in psWAT of vehicle and AA005-treated DIO mice (n=5). Data are mean ± S.D. *P□0.05, **P□0.01, ***P□0.001, NS means not significant.

Supplementary Files

This is a list of supplementary files associated with this preprint. Click to download.

- SIFiles.docx